Metrics for Analytical Expression of Transmission Line

Yuichi Tanji

Department of Reliability-based Information Systems Engineering
Kagawa University
2217-20, Hayashi-cho, Takamatsu, 761-0396 Japan

Abstract — **Analytical expression of RLCG transmission line is presented by means of *Mittag Refller's expansion*. Then, metrics for the expression are provided, where the exact poles of admittance matrix of transmission line are derived from the analytical expression and the relation between the complex pole and peak part of the frequency response is shown. When the macromodel is made from the analytical expression, the derived pole and relation allow us to determine the approximation order automatically. Further, accuracy of the macromodel is illustrated by simulations, compared with the conventional discrete model.**

1. Introduction

As the clock speed of digital system increases, the routes, ground plate, and packages on the integrated circuit and/or printed circuit board affect the system performance seriously. To avoid its worst case, the interconnect analysis of off- and on-chips using SPICE like simulator has become necessary. Since there are huge interconnects in such a system, many researchers have paid attention to the reduced-order modeling of interconnect networks in last decade [1]-[5].

When the interconnects are modeled by a distributed network (transmission line), the conventional discrete model is widely used. However, in this case, the transmission line must be finely discretized to ensure reasonable accuracy. To overcome the difficulty, the reduced-order modeling based on the Krylov subspace methods [2], [3], the moment matching techniques [4], and the matrix Padé approximation [5], have been proposed. However, these methods are not always constructed from the exact components such as poles and residues of transmission line, because the models are derived from an approximation technique.

In this paper, the analytical expression of transmission line line is presented by means of analytic consideration, that is called *Mittag Refller's expansion* [6], of the admittance matrix of transmission line. Then, metrics for the expression is provided, where the exact poles of transmission line are extracted from the analytical expression and the relationship between the derived pole and peak signal of the frequency response is considered mathematically. When the macromodel of transmission line is made from the analytical expression, the derived pole and relation allow us to determine the approximation order automatically is presented. Although the model is an asymptotic expression as the reduced-order model [1]-[5], it is composed of the exact poles and residues. Hence the proposed asymptotical expression is very compact and accurate.

This paper is organized as follows. Section II gives the analytical expression of the transmission line. Section III presents the metrics of analytical expression. In section IV, accuracy of the analytical expression is illustrated by simulations, compared with the conventional discrete model. The final section presents conclusions.

2. Analytical Expression

Consider a single-conductor lossy transmission line. The admittance matrix of transmission line is described by

$$\begin{aligned} \boldsymbol{Y}(s) &= \frac{\gamma}{R+sL}\begin{pmatrix} \coth\gamma l & -\mathrm{cosech}\,\gamma l \\ -\mathrm{cosech}\,\gamma l & \coth\gamma l \end{pmatrix} \quad (1) \\ \gamma &= \sqrt{(R+sL)(G+sC)}. \quad (2) \end{aligned}$$

The Y-matrix (1) is analytically rewritten in the infinite series of rational matrices:

$$\begin{aligned} \boldsymbol{Y}(s) = & \frac{1}{l}\frac{1}{R+sL}\begin{pmatrix} 1 & -1 \\ -1 & 1 \end{pmatrix} \\ & + \frac{2}{l}\sum_{m=1}^{\infty}\frac{G+sC}{(R+sL)(G+sC)+\left(\frac{m\pi}{l}\right)^2} \\ & \times \begin{pmatrix} 1 & (-1)^{m+1} \\ (-1)^{m+1} & 1 \end{pmatrix}. \quad (3) \end{aligned}$$

Prof) First, it is shown that the functions $\coth\gamma l$ and $\mathrm{cosech}\,\gamma l$ can be expressed in the rational functions of γ using the residues and poles.

The zeros of the denominator of $\coth\gamma l$ are described

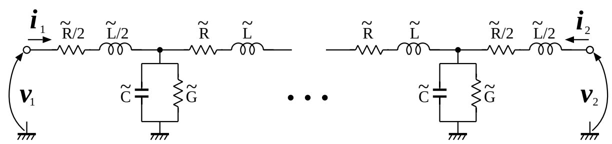

Figure 1: Discrete model of transmission line.

by

$$\gamma = \pm j\left(\frac{m\pi}{l}\right) = 0 \qquad (4)$$
$$(m = 1, 2, ...)$$

where $m = 0$ is excepted from (4) and the case is discussed later. Then, coth γl and cosech γl are expanded in the form of

$$\sum_{m=1}^{\infty}\left(\frac{k_{m,1}}{\gamma - j\left(\frac{m\pi}{l}\right)} + \frac{k_{m,2}}{\gamma - j\left(\frac{m\pi}{l}\right)}\right).$$

Since each zero of (4) is simple pole of $\coth\gamma l$, the residue $k_{m,1}$ is given from residue theorem and described by

$$k_{m,1} = \left.\frac{\cosh\gamma l}{\frac{d}{d\gamma}\sinh\gamma l}\right|_{\gamma=j\frac{m\pi}{l}l} = \frac{1}{l}. \qquad (5)$$

Also, $k_{m,2} = 1/l$. Consequently, $\coth\gamma l$ is expanded by

$$\coth\gamma l = \frac{2}{l}\sum_{m=1}^{\infty}\frac{\gamma}{\gamma^2 + \left(\frac{m\pi}{l}\right)^2}. \qquad (6)$$

As $\coth\gamma l$, $k_{m,1} = k_{m,2} = (-1)^m/l$ are given for cosech γl. Thus, cosech γl can be expressed by

$$\text{cosech }\gamma l = \frac{2}{l}\sum_{m=1}^{\infty}\frac{\gamma(-1)^m}{\gamma^2 + \left(\frac{m\pi}{l}\right)^2}. \qquad (7)$$

(6) and (7) are called *Mittag Reffler's expansion* which plays an important role on analytic elements [6].

The reason why $\gamma = 0$ has been excepted for the derivation of (6) and (7) is that $\gamma/\sinh\gamma l$ becomes indeterminate. Alternatively, we calculate the component concerned with $\gamma = 0$ by taking into account limit of γ, and the following relations

$$\lim_{\gamma\to 0}\frac{\gamma}{\sinh\gamma l} = \frac{1}{l} \qquad (8)$$
$$\lim_{\gamma\to 0}\cosh\gamma l = 1 \qquad (9)$$

are given. Using (8) and (9), (1) yields

$$\frac{1}{l}\frac{1}{R+sL}\begin{pmatrix} 1 & -1 \\ -1 & 1 \end{pmatrix}. \qquad (10)$$

From (6), (7), and (10), the analytical expression of transmission line is given by (3).

□

3. Metrics of Analytical Expression

3.1. Poles

The exact poles of transmission line are calculated from (3). The real pole is described by

$$p_s = -\frac{R}{L}. \qquad (11)$$

The complex conjugate pair is described by

$$p_{c,m} = \frac{\alpha + j\beta}{2LC}, \quad p_{c,m}^* = \frac{\alpha - j\beta}{2LC} \qquad (12)$$

where

$$\alpha = -(RC + LG)$$
$$\beta = \sqrt{4LC\left\{RG + \left(\frac{m\pi}{l}\right)^2\right\} - (RC+LG)^2}.$$

Although it is impossible to compare the poles (11) and (12) with the poles of discrete model of transmission line completely, we show the difference when the transmission line is modeled by one T-section. The model of transmission line is shown in Fig. 1. Assuming n divisions, the passive elements of the model is represented by

$$\tilde{R} = \frac{Rl}{n}, \quad L = \frac{Ll}{n}, \quad C = \frac{Cl}{n}, \quad G = \frac{Gl}{n}. \qquad (13)$$

When $n = 1$, (1,1) element of the admittance matrix is described by

$$y_{11}(s) = \frac{1}{l}\frac{1}{R+sL} + \frac{1}{l}\frac{G+sC}{(G+sC)(R+sL) + \left(\frac{2}{l}\right)^2}. \qquad (14)$$

The single pole of (14) is the same with the exact pole (11), but the complex poles are different from the exact ones. In the next section, it is shown by simulation that with the increase in n, the complex poles of discrete model approaches the exact ones.

3.2. Peak Location

In the reduced-order modeling [1]-[5], it is very difficult to decide the approximation order. The number of division for discrete model is not easy to decide, too. Fortunately, the poles (11) and (12) are analytically derived. When (3) is truncated by finite terms and used as the macromodel of transmission lines, therefore, we can use the poles to determine the approximation order automatically.

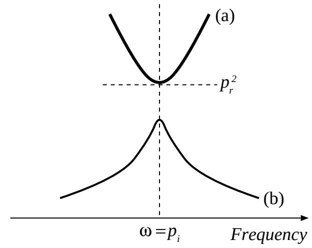

Figure 2: Profile of (16). (a) $p_r^2 + (\omega - p_i)^2$. (b) $1/\sqrt{p_r^2 + (\omega - p_i)^2}$.

From (12), the following relation

$$\beta \propto m \tag{15}$$

is satisfied, which means that when the finite terms in (3) is considered as $m = 1, \ldots, M$ it yields the reduced-order model covering the lower frequency part. So, let us investigate the influences of a complex pole p on the frequency response at the image axis of complex s, i.e., $s = j\omega$.

The amplitude of the function $k/(j\omega - p)$ is described by

$$\mathrm{Amp}\left(\frac{k}{j\omega - p}\right) = \sqrt{\frac{k_r^2 + k_i^2}{p_r^2 + (\omega - p_i)^2}} \tag{16}$$

where $p = -p_r + jp_i$ ($p_r, p_i > 0$) is a complex pole and $k = k_r + jk_i$ is the residue. The function (16) whose profile is shown in Fig. 2 has the peak at

$$f_i = p_i/(2\pi). \tag{17}$$

Therefore, we can automatically decide the truncated terms of (3) by setting an frequency f_c. When the imaginary part of a pole is beyond f_c, the summation (3) is truncated by the terms.

4. Simulations

To estimate accuracy of analytical expression, the transmission line with the parameters, $R = 0.5[\Omega/\mathrm{cm}]$, $L = 10.0[nH/\mathrm{cm}]$, $C = 0.004[nF/\mathrm{cm}]$, $G = 0.0005[S/\mathrm{cm}]$, $l = 1[\mathrm{cm}]$, was analyzed. First, the exact poles of the transmission line were calculated following (11) and (12). The real pole was $p_r = -0.05 \times 10^9$. All the real parts of the complex poles were equal to each other and $\mathrm{Re}[p_i] = -0.0875 \times 10^9$ ($i = 1, 2, \ldots$). For a comparison, the poles of the discrete model shown in Fig. 1 were computed by eigen decomposition routine. As the exact poles, all the real parts of the complex poles were -0.0875×10^9. Therefore, we show the imaginary parts of them only as shown in Fig. 3, where the ones with positive imaginary parts are shown, because all poles are complex conjugate. In this figure, the horizontal and horizontal axes show imaginary part of pole and m in (12), respectively.

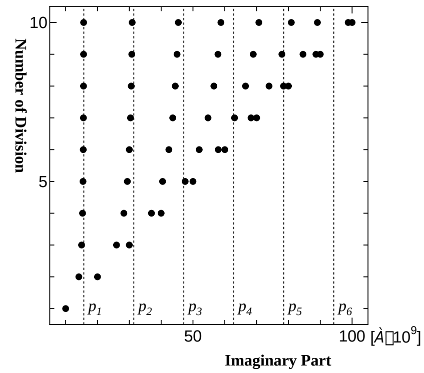

Figure 3: Imaginary part of poles for example.

Consider the discrete model with n T sections. Assume the complex poles as $\hat{p}_{c,i,n}$, and $\hat{p}^*_{c,i,n}$ ($i = 1, \ldots, n$), where symbol "*" implies complex conjugate operator. Then, the result shown in Fig 3 suggests

$$\lim_{n\to\infty} \hat{p}_{c,i,n} = p_{c,i}, \qquad \lim_{n\to\infty} \hat{p}*_{c,i,n} = p^*_{c,i},$$
$$(i = 1, \ldots, n)$$

that is, the poles of discrete model converges to the exact ones when the line is divided infinitely.

Next, the frequency responses of the macromodel

$$\begin{aligned} \boldsymbol{Y}(s) &= \frac{1}{l}\frac{1}{R+sL}\begin{pmatrix} 1 & -1 \\ -1 & 1 \end{pmatrix} \\ &+ \frac{2}{l}\sum_{m=1}^{3}\frac{G+sC}{(R+sL)(G+sC)+\left(\frac{m\pi}{l}\right)^2} \\ &\times \begin{pmatrix} 1 & (-1)^{m+1} \\ (-1)^{m+1} & 1 \end{pmatrix} \end{aligned}$$

obtained by truncating (3) were computed as shown in Fig. 4, where "*asymptotic*" and "*exact*" indicate the responses of the finite order model in (3) and the exact response, respectively. As suggested in the previous section, frequency response of transmission line has a peak part at the frequency of (17) to a pole p. This is observed from Fig. 4. On the other hand, the frequency responses to the discrete models are shown in Fig. 5. As we can see, the finite order approximation in (3) gives a better approximation result than the one of the discrete model as shown in Fig. 5(a), where the same number of poles are provided in both models. When the number of division increases, accuracy of the discrete model is comparable with the analytical expression as shown in Fig. 5(b).

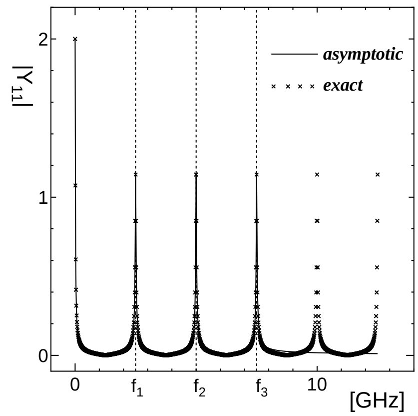

Figure 4: Y parameter for example.

However, a secondary problem occurs there. Certainly, the frequency response to the discrete model approaches the exact one in the low frequency portion as the number of division increases. However, the high frequency portion remain inaccurate. The influence is never removed even if the transmission line is finely discretized. That is the reason why discrete model of transmission lines brings a fault ringing. In contrast to the discrete model, the proposed macromodel does not have redundant and inaccurate portions, exactly, the frequency response is dumped in the uncovered region. Therefore, a fault ringing would be generated different from the discrete model and it can be widely used as interconnect models instead of the discrete one.

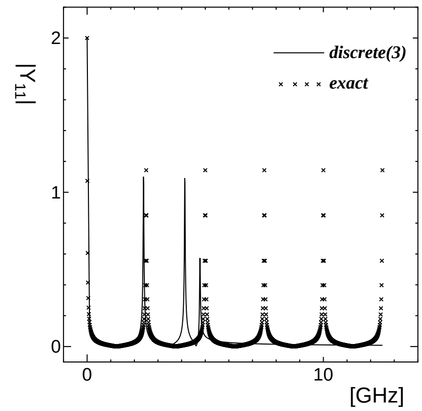

(a)

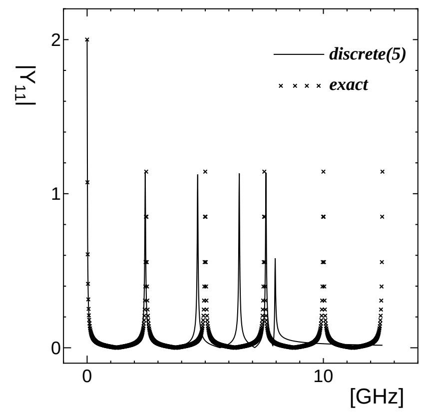

(b)

Figure 5: Y parameter of the discrete model. (a) 3 sections case. (b) 5 sections case.

5. Conclusions

Metrics of the analytical expression of RLCG transmission line derived from the *Mittag Reffler's expansion* [6] have been presented. From the expression, the exact poles of transmission line are given. Next, the relation between the complex pole and the peak signal of the frequency response is shown. If the macromodel of transmission line is made from the analytical expression, the relation allows us to determine the approximation order automatically. Further, it is illustrated by simulations that the macromodel obtained from the analytical expression is superior to the conventional discrete model. We will present the circuit model of the macromodel in near future.

References

[1] L. T. Pillage and R. A. Rohrer, "Asymptotic waveform evaluation for timing analysis," *IEEE Trans. Computer-Aided Design*, vol. 9, no. 4, pp. 352-366, Apr. 1990.

[2] P. Feldmann and R. W. Freund, "Efficient linear analysis by padé approximation via the Lanczos process," *IEEE Trans. Computer-Aided Design*, vol. 14, no. 5, pp. 639-649, May 1995.

[3] A. Odabasioglu, M. Celik, and L. T. Pilleggi, "Prima: passive reduced-order interconnect macromodeling algorithm," *IEEE Trans. Computer-Aided Design*, vol. 17, no. 8, pp. 645-654, Aug. 1998.

[4] Q. Yu, J. M. L. Wang, and E. S. Kuh, "Passive multipoint moment matching model order reduction algorithm on multiport distributed interconnect networks," *IEEE Trans. Circuits & Systems-I*, vol. 46, no. 1, pp. 140-160, Jan. 1999.

[5] A. Dounavis, X. Lin, M. S. Nakhla, and R. Achar, "Passive closed-form transmission-line model for general-purpose circuit simulators," *IEEE Trans. Microwave Theory Tech.*, vol. 47, no. 12, pp. 2450-2459, Dec. 1999.

[6] A. Escassut, *Analytic Elements in p-Adic Analysis*, World Scientific, 1995.